COMPDYN 2015
5th ECCOMAS Thematic Conference on
Computational Methods in Structural Dynamics and Earthquake Engineering
M. Papadrakakis, V. Papadopoulos, V. Plevris (eds.)
Crete Island, Greece, 25–27 May 2015

DOUBLE-LAYER PLATFORM OF HIGH PERFORMANCE COMPUTING FOR DAMAGE PREDICTION OF RC BUILDINGS SUBJECT TO EARTHQUAKE AND SUBSEQUENT TSUNAMI IN A TARGET AREA

P. Latcharote[1] and Y. Kai[2]

[1] Department of Infrastructure Systems Engineering, Kochi University of Technology, Japan
e-mail: panoname@hotmail.com

[2] Department of Infrastructure Systems Engineering, Kochi University of Technology, Japan
e-mail: kai.yoshiro@kochi-tech.ac.jp

Keywords: Damage Prediction, Earthquake and Subsequent Tsunami, Sequential Earthquake and Tsunami Simulation, Double-Layer Platform, CUDA.

Abstract. *For tsunami scenarios, evaluation of tsunami load acting each building depends on surrounding circumstance. Therefore, modeling of all buildings in a target area is important for damage prediction from earthquake and subsequent tsunami. In this study, sequential earthquake and tsunami simulation was developed to predict structural damage from earthquake and subsequent tsunami by means of the application in Integrated Earthquake Simulation (IES). Since IES can simulate only earthquake scenarios with bean-column frame models, IES was modified for input tsunami load acting on a proposed wall-frame model in order to simulate tsunami scenarios using predicted data of tsunami inundation depth. A target area in Kochi city was selected to simulate an earthquake and tsunami scenario because this area has many public buildings and is important for economic activities. A double-layer platform of high performance computing was proposed to simulate this earthquake and tsunami scenario with parallel processing on CPUs and GPUs. The results of sequential earthquake and tsunami simulation show that three-story RC buildings had a significant risk that maximum drift ratio could occur during sequential tsunami response. However, maximum drift ratio from sequential tsunami response was still less than 0.3% in which structural damage didn't occur obviously. For the worst case scenario that tsunami inundation depth was double, structural damage from sequential tsunami response was much more serious than that of the normal-case scenario in which maximum drift ratio was less than 5% for a four-story RC building. In addition, it was found that low-rise buildings (three- to seven-story) had a significant risk that maximum drift ratio was higher than 1% during sequential tsunami response. The results of sequential earthquake and tsunami simulation can be used to construct further prevention measures.*

1 INTRODUCTION

Based on past experience in the Great East Japan earthquake and tsunami, many buildings in Tohoku area were seriously damaged by earthquake and subsequent tsunami. In the future, severe damage as serious as the previous earthquake and tsunami may occur in other area of Japan, such as Tokai, Tonankai, Nankai area. In order to reduce the loss of human life in future earthquake and tsunami, damage prediction is a key role for constructing prevention measure and raising awareness of people. For damage prediction in a target area, computer technology has been applied to simulate earthquake scenarios, such as Integrated Earthquake Simulation (IES) [1-7]. Integrated Earthquake Simulation (IES) is an earthquake simulation tool for predicting and illustrating structural damage of all buildings in the target area simultaneously in selected earthquake scenarios. Based on Geographic Information System (GIS) data in Figure 1(a), thousands of buildings in the target area are modeled to polygon shapes in Figure 1(b) from building shape and height. Based on building design code, Common Modeling Data (CMD) is a modeling approach to convert a polygon shape in Figure 2(a) as a structural model in Figure 2(b), consisting of beam and column elements including section and material properties of each element. In Figure 1(c), nonlinear structural analysis of all buildings in the target area is performed to predict structural damage and then illustrate structural damage of all buildings simultaneously as shown in Figure 1(d).

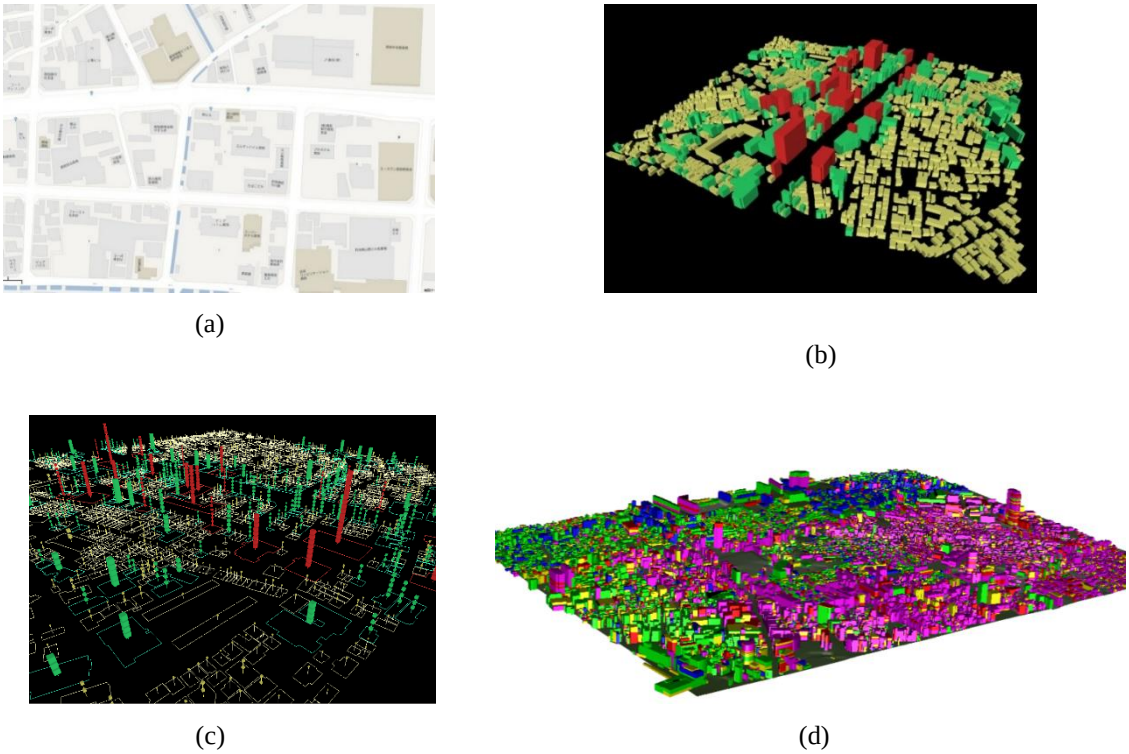

(a) (b) (c) (d)

Figure 1: Integrated Earthquake Simulation [4]

For a target area, structural damage of each building is predicted from the results of nonlinear structural analysis. Object-Based Structural Analysis (OBASAN), a structural analysis program, which has been developed by our laboratory, is proposed to perform nonlinear structural analysis in IES. Therefore, there are two main parts in this study: the first part is IES for building modeling and the second part is OBASAN for nonlinear structural analysis. For thousands of buildings in the target area, IES can visualize structural damage to raise awareness of disaster prevention among people in that area. Since high performance computing

(HPC) is a key role to carry out a large number of buildings in the target area, OpenMPI application has been applied to IES in order to enable parallel processing on the Central Processing Units (CPUs).

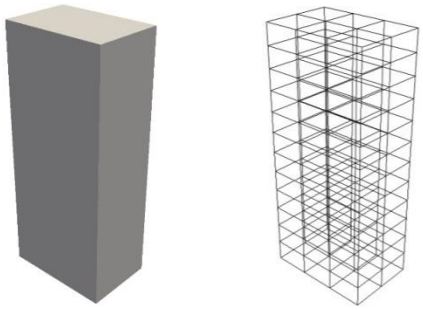

(a) (b)

Figure 2: Common Modeling Data (CMD) [10]

2 DOUBLE-LAYER PLATFORM OF HIGH PERFORMANCE COMPUTING

For damage prediction in a target area, thousands of buildings are modeled to perform nonlinear structural analysis. Since high performance computing (HPC) is a key role to carry out a large number of buildings in the target area, OpenMPI application has been applied to IES in order to enable parallel processing on the Central Processing Units (CPUs) for building modeling of all buildings [1-7]. In this study, a double-layer platform of HPC was proposed to simulate earthquake and tsunami scenarios in a reasonably short time. Since OBASAN has been developed by C++ programing language, CUDA application was applied to OBASAN in order to enable parallel processing on the Graphic Processing Units (GPUs) for nonlinear structural analysis of a building. Therefore, HPC was achieved by a double layer of parallel processing on CPUs and GPUs as shown in Figure 3.

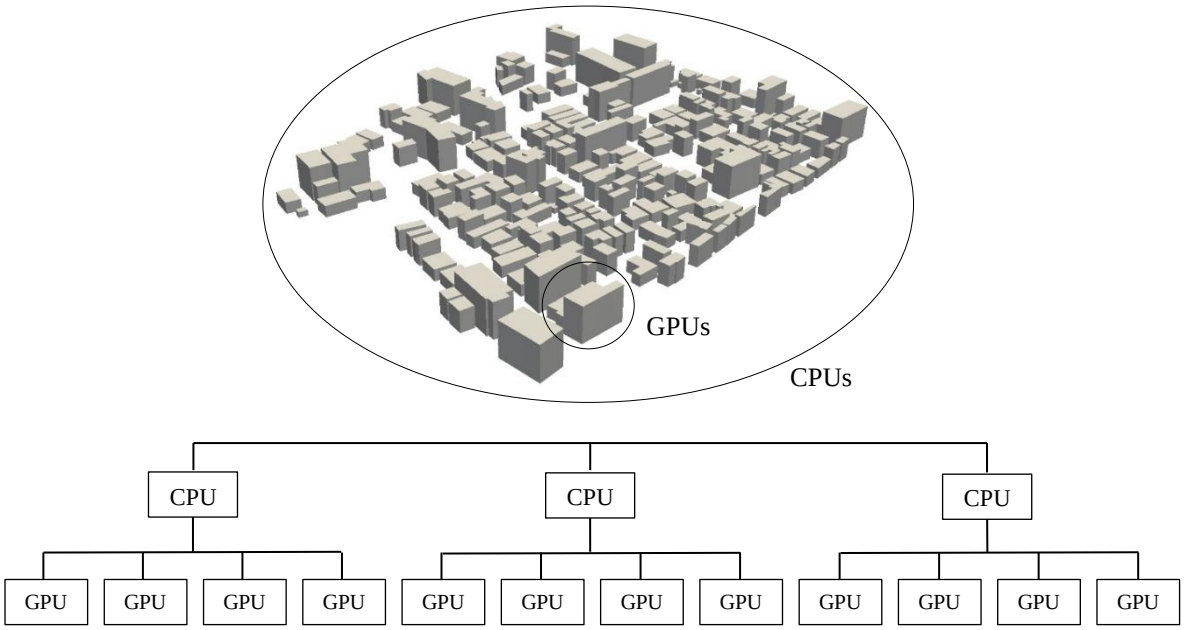

Figure 3: A proposed double layer of parallel processing on CPUs and GPUs

CUDA application is one of General-Purpose computing on Graphic Processing Units (GPGPUs) which has high capability to carry out a large amount of data and a large number

of simple calculation [11-12]. For nonlinear structural analysis in OBASAN, it was found that most of execution time was occupied by matrix operation Ax = b, so CUDA application was used to solve this matrix operation at every analysis steps on GPUs using CUBLAS and CUSPARSE library.

3 DAMAGE PREDICTION FROM EARTHQUAKE AND TSUNAMI

In this study, damage prediction of all RC buildings in a target area from earthquake and subsequent tsunami was proposed by means of the application in IES. Since IES can simulate only earthquake scenarios, IES was modified to input tsunami load acting on each building in order to simulate tsunami scenarios using data of tsunami inundation depth provided by Japan Cabinet Office (JCO). In IES, evaluation of tsunami load was included for all RC buildings as the same approach as earthquake scenarios and new building modeling was proposed to perform nonlinear structural analysis of each RC building subject to tsunami load.

3.1 Evaluation of tsunami load

For earthquake scenarios, the wave data of strong ground motion was input to all RC buildings as same as previous in IES. For tsunami scenarios, the predicted data of tsunami inundation depth was input to all RC buildings in order to evaluate tsunami load, which also depends on surrounding circumstance in the target area. However, in this study, tsunami load was calculated by means of triangle distribution of hydrostatic pressure recommend by JCO shown in Figure 4. Due to considering effect of impact force, tsunami load in Eq. (1) was magnified by a factor, which can vary from 1.0 to 3.0 depending on surrounding circumstance.

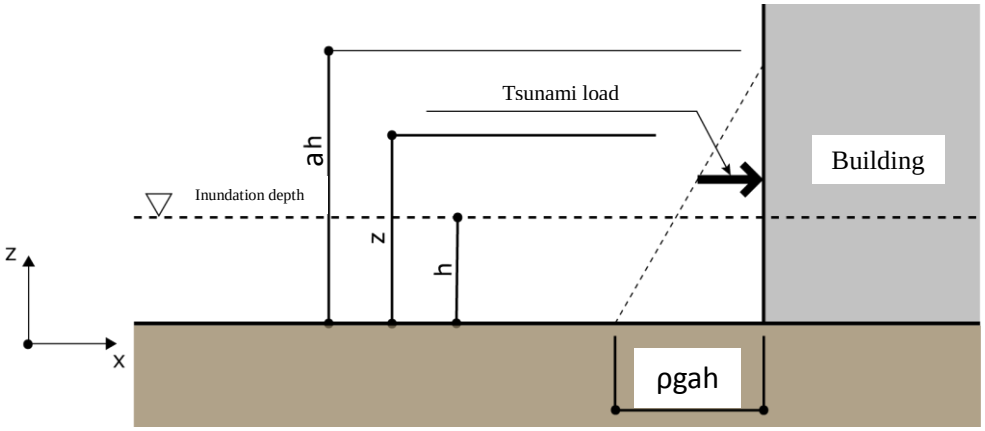

Figure 4: Triangle distribution of hydrostatic pressure (JCO)

$$q_z = \rho_s g(ah - z) \tag{1}$$

in which q_z: hydrodynamic force, ρ_s: density of salt water = 1128 kg/m3, g: gravitational acceleration = 9.81 m/s^2, h: inundation depth, z: height from ground level ($0 \le z \le h$), a: impact factor ($1.0 \le a \le 3.0$)

Figure 5 shows the location of RC buildings (grey colour) and wooden houses (green colour) in a target area. Unless tsunami inundation depth and flow velocity, tsunami load acting on each building also depended on tsunami direction to this area, building location from coastal line, and building arrangement in this area. Focusing on one RC building in Figure 5, tsunami load can be reduced by surrounding buildings and environment, whereas tsunami

load can be increased by wooden debris from collapsed houses. As can be seen in Figure 5, it shows that surrounding circumstance had a significant effect on evaluation of tsunami load for all RC buildings in the target area.

Figure 5: Location of RC buildings and wooden houses in a target area

In Table 1, the a factor was investigated to evaluate tsunami load in Eq. (1) based on damage observation after the 2011 Great East Japan earthquake [13]. As shown in Table 1, the investigation of the a factor was separated to only two cases: area with structures to reduce tsunami load and area without structures to reduce tsunami load.

Coefficient	Area with structures to reduce tsunami load	Area without structures to reduce tsunami load
a	1.0	≥ 1.7

Table 1: The a factor based on damage observation after the 2011 Great East Japan earthquake [13]

The direction of tsunami load acting on each RC building in this study was assumed in both x- and y- directions as shown in Figure 6.

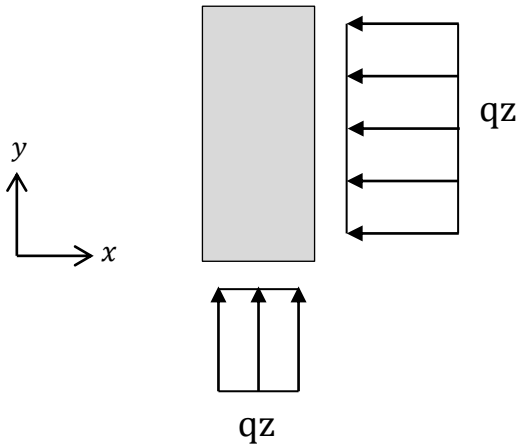

Figure 6: The direction of tsunami load acting on each RC building in a target area

3.2 Proposed building modeling

In IES, Common Modeling Data (CMD) is a modeling approach to convert a polygon shape as a structural model, consisting of beam and column elements, based on building design code. As the first part of the simulation in this study, building modeling in CMD was modified to include wall elements to a structural model in order to perform nonlinear structural analysis of RC buildings subject to tsunami load. As shown in Figure 7, a polygon shape in Figure 7(a) was converted to a structural model in Figure 7(b), consisting of beam, column, wall elements.

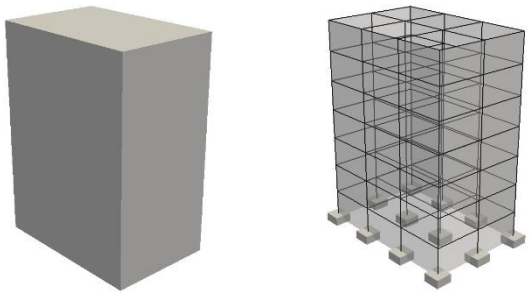

(a) (b)

Figure 7: Proposed building modeling

Since tsunami load was a distributed pressure acting on outside of RC buildings as shown in Figure 4 and Figure 6, wall elements were arranged to outside frames for resisting a distributed pressure of tsunami load. In order to apply this proposed building modeling of wall elements as the concept of CMD, wall elements were arranged to all outside frames of RC buildings covering building surface as wall cladding shown in Figure 8. For this proposed building modeling, macro plate model was applied to represent wall elements in the structural model.

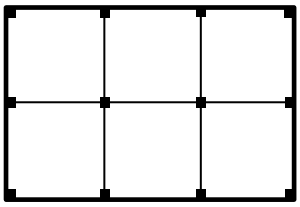

Figure 8: Common Modeling Data for wall elements

In conclusion, all RC buildings in a target area were represented as a structural model, consisting of beam, column and wall elements, in order to perform nonlinear structural analysis of each RC building subject to earthquake and subsequent tsunami.

4 SEQUENTIAL ANALYSIS FROM EARTHQUAKE AND TSUNAMI

Object-Based Structural Analysis (OBASAN), a structural analysis program, which has been developed by our laboratory, was proposed to perform nonlinear structural analysis as the second part of the simulation. For earthquake and tsunami scenarios, strong ground motion shakes all buildings and causes some structural damage to all buildings in a target area. Subsequently, a tsunami reaches the target area and tsunami load causes more structural damage to buildings. In OBASAN, RC buildings were analyzed by inputting a sequential load of earthquake and tsunami as shown in Figure 9. In the case of earthquake in Figure 9(b), dy-

namic structural response analysis was performed to predict structural damage of each building, which was subject to strong ground motion. Sequentially, static pushover analysis was performed to predict more structural damage to each building, which was subject to tsunami load in Figure 9(c).

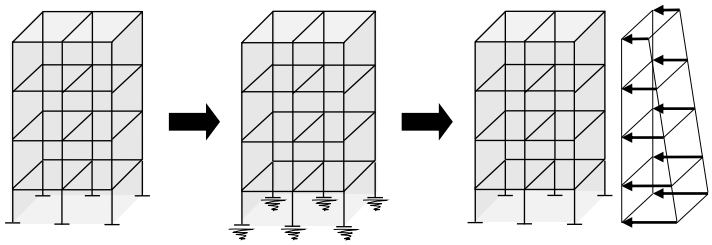

(a) (b) (c)

Figure 9: Sequential analysis of earthquake and tsunami

In order to simulate sequential behavior of earthquake and tsunami response, nonlinear structural analysis was performed by means of the same hysteresis model shown in Figure 10. The red line represents nonlinear structural analysis in earthquake scenario and the blue line represents nonlinear structural analysis in tsunami scenario. During an earthquake, nonlinear structural analysis starts from point A and moves along the red line of hysteresis loop. Then, nonlinear structural analysis stops at point B and some structural damage occurred from earthquake scenario. During tsunami scenario, nonlinear structural analysis starts from point B and moves along the blue line. Then nonlinear structural analysis stops at point C and more structural damage might occur from tsunami scenario.

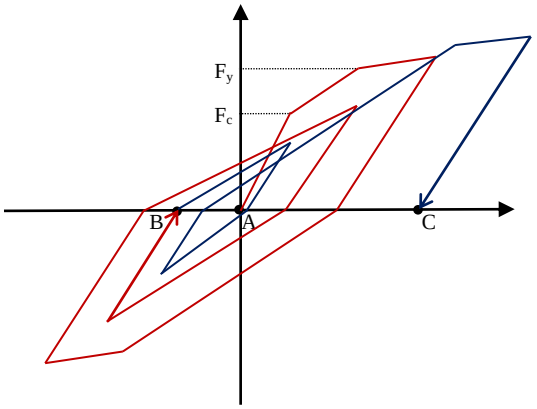

Figure 10: Hysteretic loop for earthquake and subsequent tsunami

5 EARTHQUAKE AND TSUNAMI SCENARIO IN KOCHI CITY

In this study, a target area in Kochi city was selected to simulate an earthquake and tsunami scenario as shown in Figure 11. This selected target area is in the center of Kochi city which has many public buildings and is important for economic activities. For damage prediction in this target area, an earthquake and tsunami scenario was simulated from input data, such as GIS data for building modeling, wave data of strong ground motion, and predicted data of tsunami inundation depth.

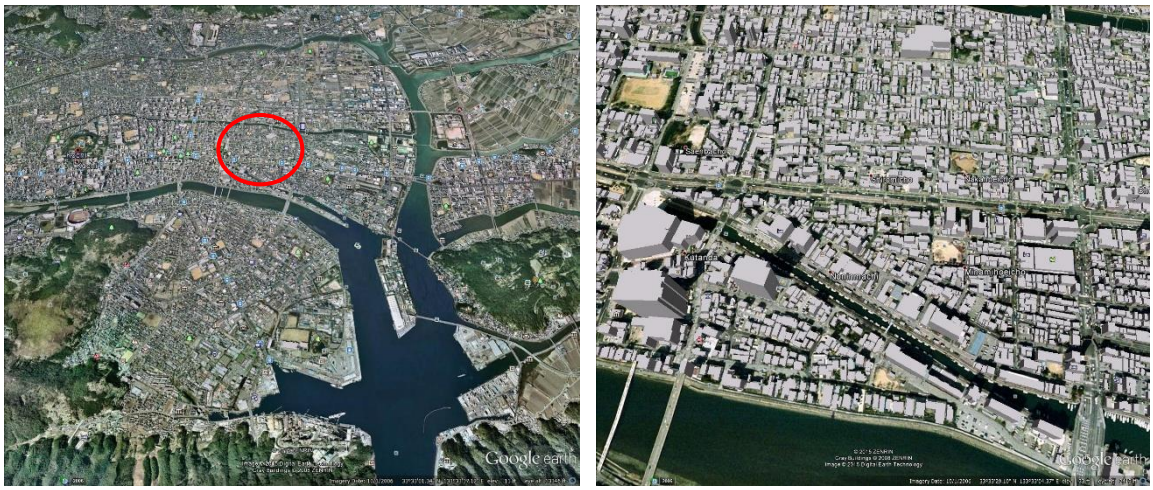

Figure 11: A selected target area in Kochi city

5.1 GIS data for building modeling

Figure 12 shows GIS data of this selected target area. In GIS data, building dimensions and number of floors were used to generate building shapes of all buildings as shown in Figure 13(a) in which each building can be classified to RC buildings, steel buildings, and wooden houses.

Figure 12: GIS data of this target area

In Figure 13(a), this selected target area had 480 RC buildings (grey color) and 1311 wooden houses (green color). Since damage prediction of all RC buildings in a target area from earthquake and subsequent tsunami was proposed in this study, 480 RC buildings in Figure 13(b) were applied to simulate an earthquake and tsunami scenario.

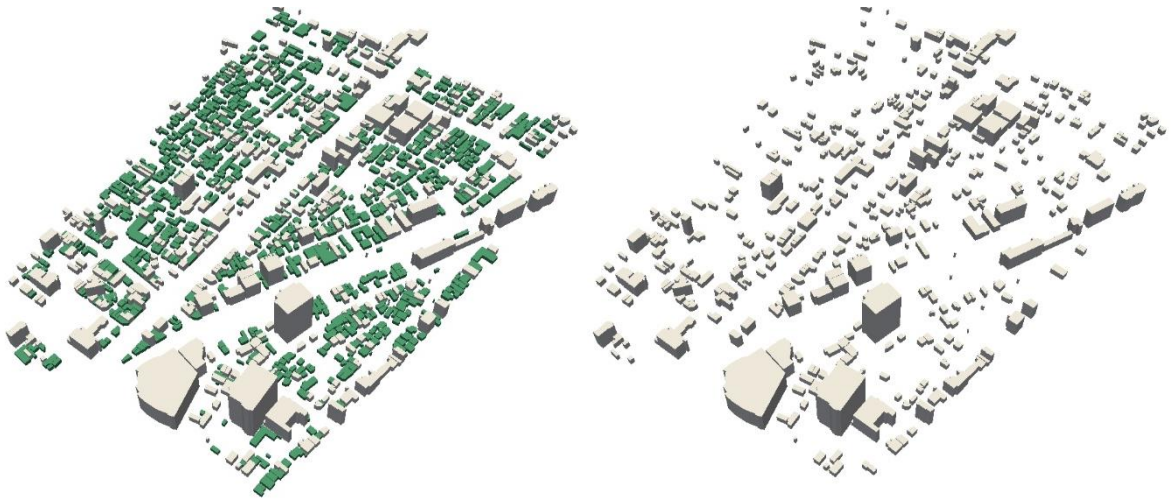

(a) (b)

Figure 13: Building shapes from GIS data

5.2 Wave data of strong ground motion

The wave data of Kochi city has been developed by a study group of the Great Nankai earthquake model from Japan Cabinet Office (JCO) in 2012. This selected target area was separated to north zone and south zone according to two source data of earthquake model as shown in Figure 14.

Figure 14: Two separated zone for two source data of earthquake model

Figure 15 shows the wave data of strong ground motion for this selected target area. The wave data in Figure 15(a) was applied to all RC buildings in south zone and the wave data in Figure 15(b) was applied to all RC buildings in north zone. As can be seen in Figure 15(a) and 15(b), three motion components in the east-west, north-south, and up-down direction (EW, NS, and UD respectively) have been developed in a wave form of ground acceleration in which shear wave velocity (Vs) is equal to 300 m/s. The peak ground acceleration of north zone in all EW, NS, and UD directions is higher than that of south zone.

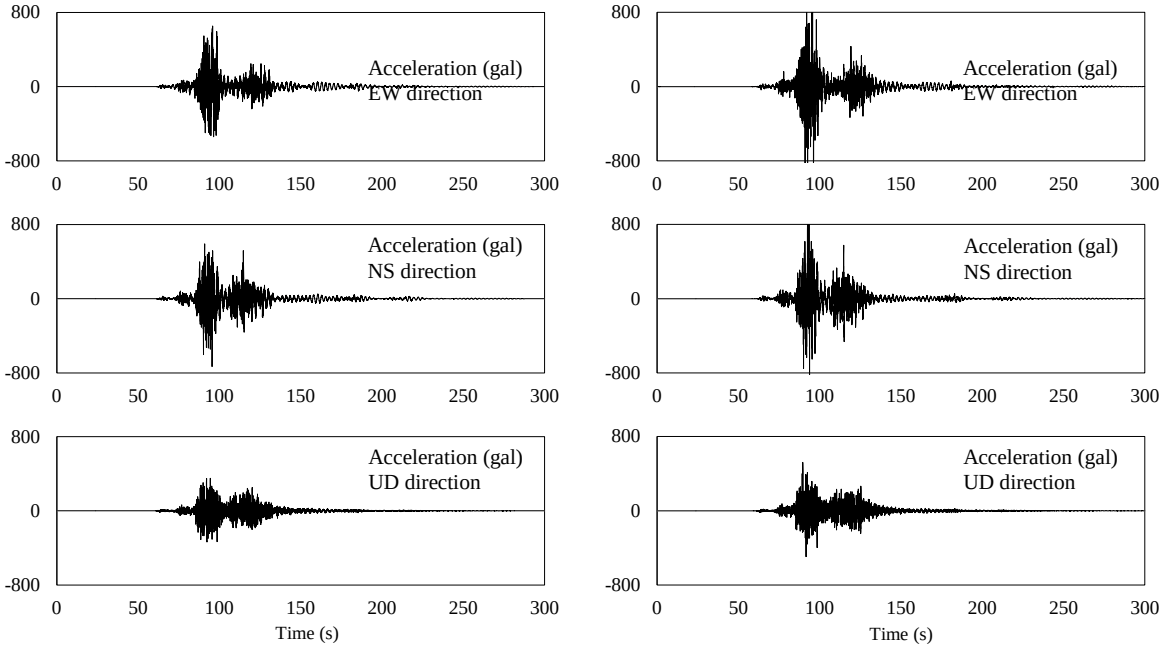

(a) (b)

Figure 15: The wave data of strong ground motion (JCO, 2012)

5.3 Predicted data of tsunami inundation depth

Japan Cabinet Office (JCO) has studied and predicted tsunami inundation depth in future earthquake and tsunami for all risk area in Japan. Based on tsunami hazard map provided by JCO, this selected target area was divided to seven area shown in Figure 16 consist of three area (N1, N2, and N3) in north zone and four area (S1, S2, S3, and S4) in south zone for tsunami inundation data in time history. In this target area, the maximum inundation depth was varied from 2.0 m to 3.5 m.

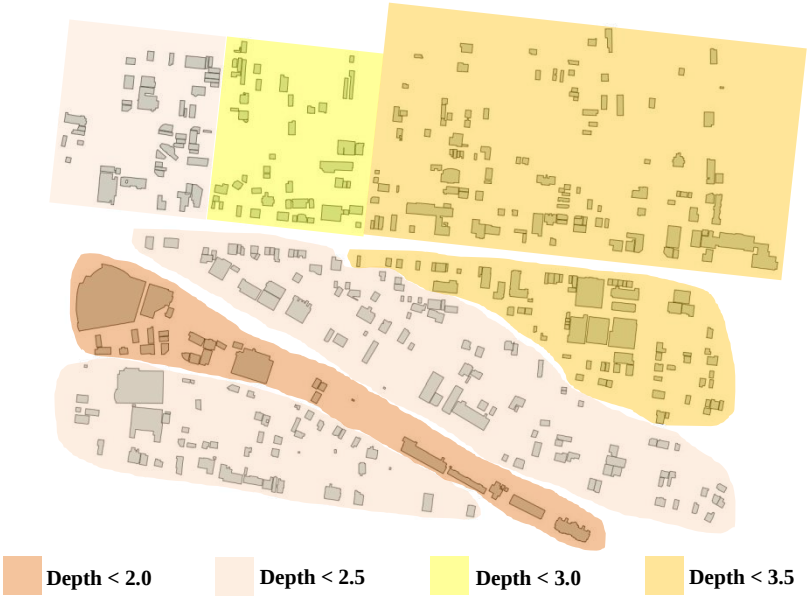

Figure 16: Seven divided area for tsunami inundation data

Figure 17 shows the predicted data of tsunami inundation depth for this selected target area. The inundation data in Figure 17(a) was used to evaluate tsunami load for all RC buildings in south zone and the inundation data in Figure 17(b) was used to evaluate tsunami load for all RC buildings in north zone.

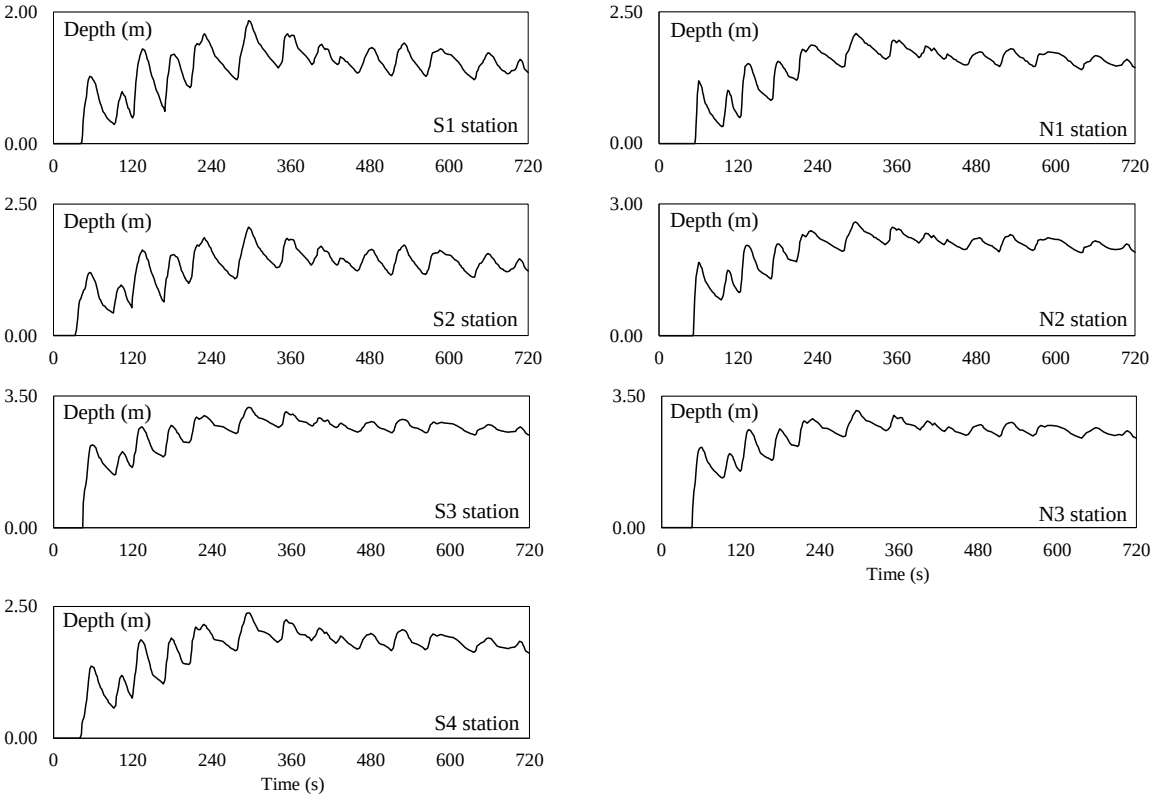

Figure 17: Predicted inundation depth at each station (Kochi Prefecture Office)

6 RESULTS OF SEQUENTIAL EARTHQUAKE AND TSUNAMI SIMULATION

The results of sequential earthquake and tsunami simulation can be visualized as shown in Figure 18. For each RC building, structural damage can be predicted by means of maximum story drift ratio.

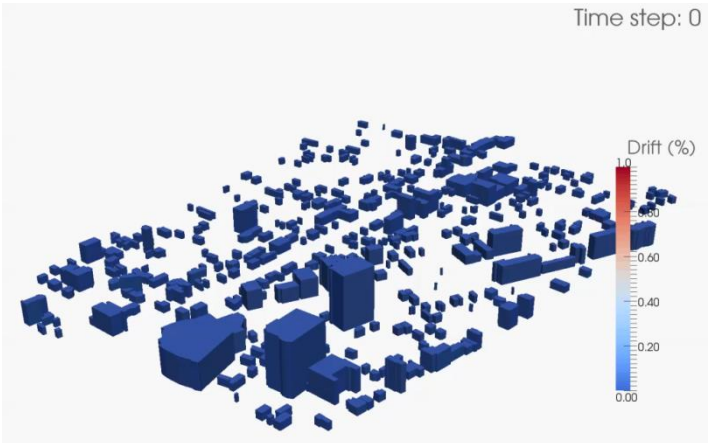

Figure 18: Visualization of damage prediction

For each RC building, the results of story displacement at 1st floor in x- and y- directions can be obtained as shown in Figure 19. Figure 19(a) shows the results of a three-story RC building and Figure 19(b) shows the results of an eight-story RC building. As can be seen in Figure 19, sequential tsunami response in y-direction had a significant effect on a three-story RC building. In addition, residual displacement occurred from earthquake response in x-direction. Therefore, the effect of sequential tsunami response depended on building height and also the direction of tsunami load.

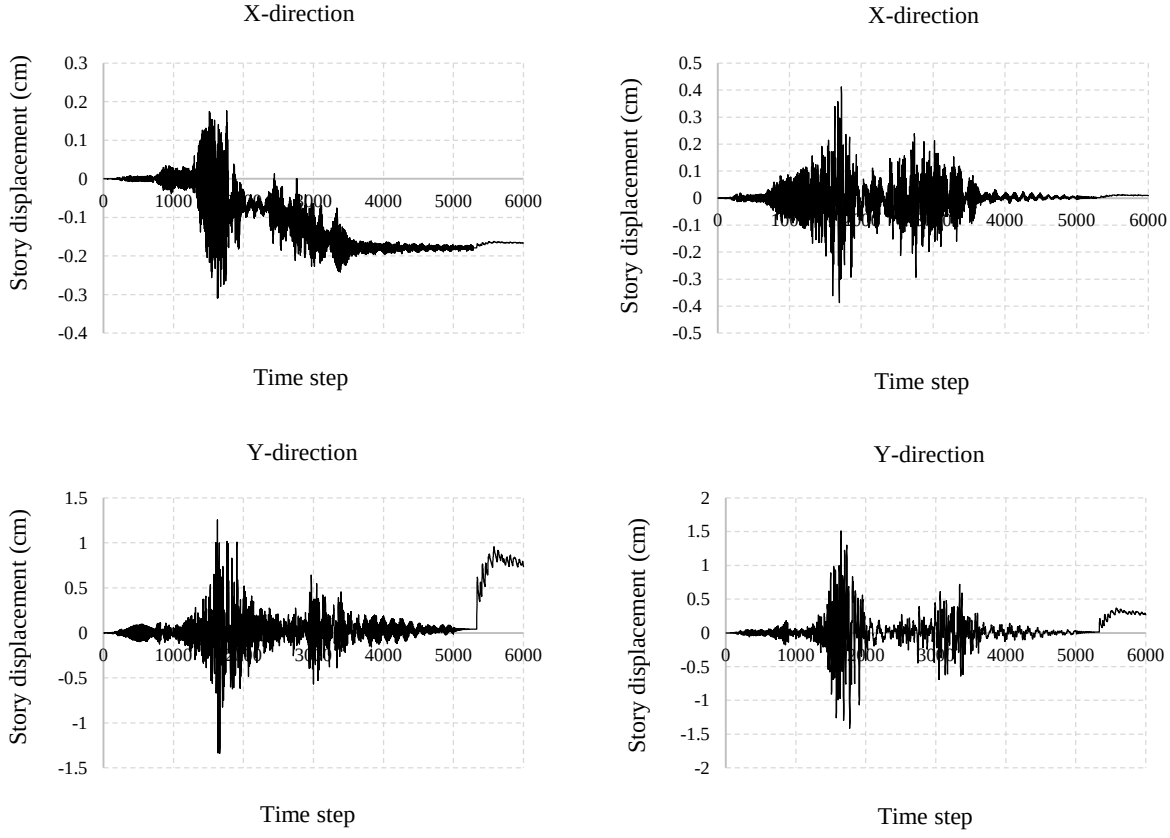

Figure 19: Story displacement at 1st floor

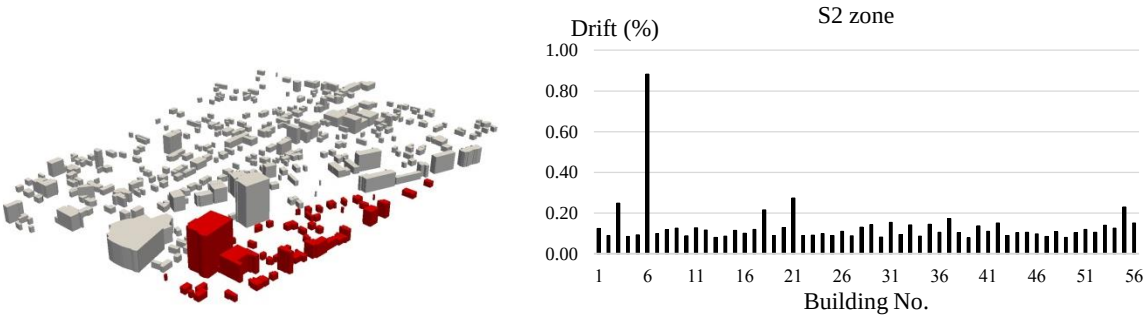

Figure 20: Maximum story drift ratio for zone S2

Figure 20 shows the results of maximum story drift ratio for each RC building in zone S2. For each RC building in Figure 20, number of floors, maximum story drift ratio, occurrence during earthquake response or sequential tsunami response, and location of maximum story drift can be seen in Appendix I.

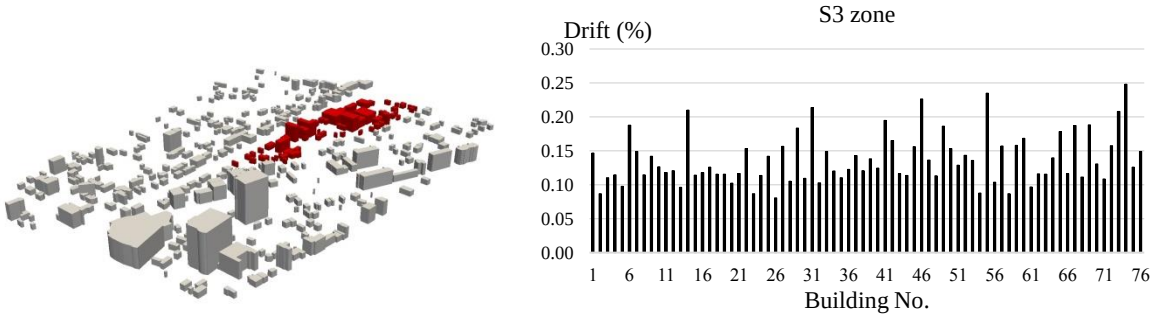

Figure 21: Maximum story drift ratio for zone S3

Figure 21 shows the results of maximum story drift ratio for each RC building in zone S3. For each RC building in Figure 21, number of floors, maximum story drift ratio, occurrence during earthquake response or sequential tsunami response, and location of maximum story drift can be seen in Appendix II.

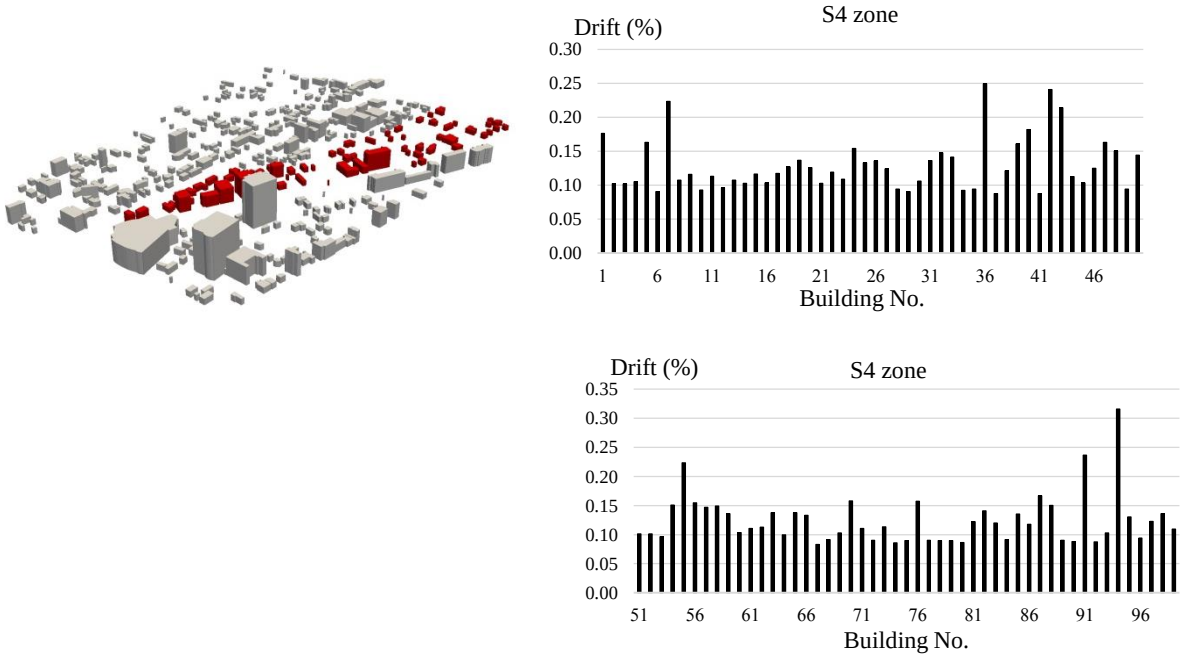

Figure 22: Maximum story drift ratio for zone S4

Figure 22 shows the results of maximum story drift ratio for each RC building in zone S4. For each RC building in Figure 22, number of floors, maximum story drift ratio, occurrence during earthquake response or sequential tsunami response, and location of maximum story drift can be seen in Appendix III.

Table 2 shows number of RC buildings in which maximum story drift ratio occurred during earthquake response and sequential tsunami response.

Zone	Number of RC buildings	Max drift during earthquake	Max drift during tsunami
N1	50	50	0
N2	51	50	1
N3	114	111	3
S1	31	24	7
S2	56	40	16
S3	76	45	31
S4	99	71	28
Total	477	391 (81.97%)	86 (18.03%)

Table 2: Number of RC buildings for maximum story drift ratio

7 THE WORSE-CASE SCENARIO

Figure 23 shows sequential earthquake and tsunami simulation assuming the worst-case scenario by increasing double of tsunami inundation depth. From the visualization of results in Figure 23, maximum story drift ratio can occur less than 5% in which that of maximum story drift ratio in Figure 18 can occur less than 1%.

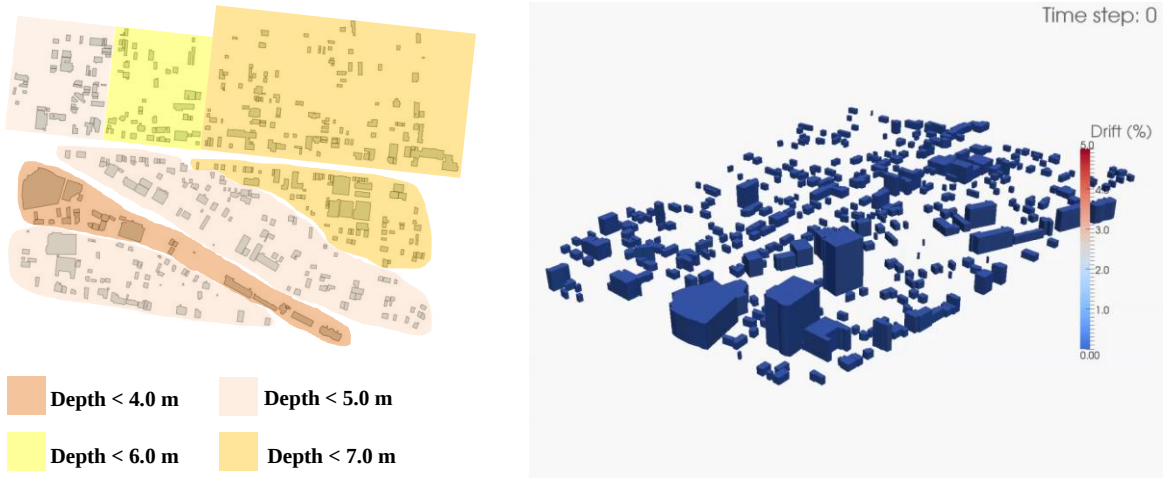

Figure 23: The worst-case scenario by increasing double of tsunami inundation depth

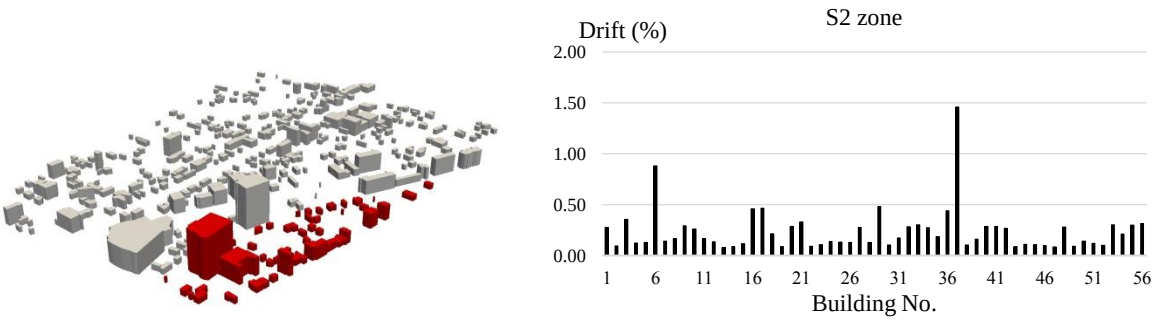

Figure: 24 Maximum story drift ratio for zone S2 (worst case)

Figure 24 shows the results of the worst-case scenario for each RC building in zone S2. For each RC building in Figure 24, number of floors, maximum story drift ratio, occurrence

during earthquake response or sequential tsunami response, and location of maximum story drift can be seen in Appendix IV.

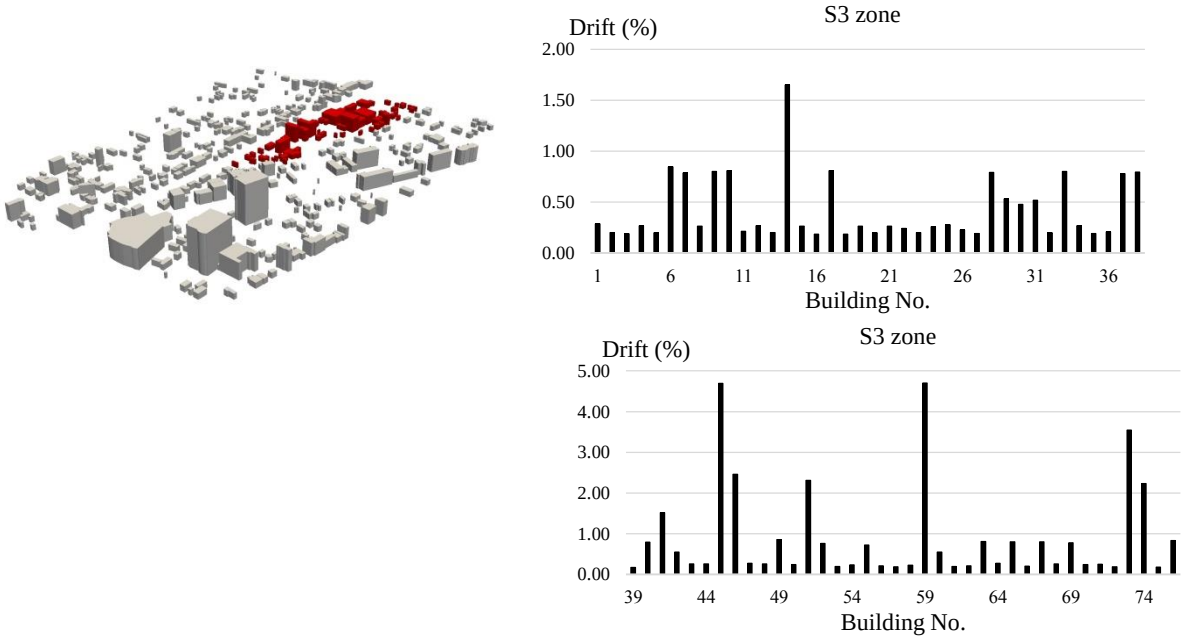

Figure 25: Maximum story drift ratio for zone S3 (worst case)

Figure 25 shows the results of the worst-case scenario for each RC building in zone S3. For each RC building in Figure 25, number of floors, maximum story drift ratio, occurrence during earthquake response or sequential tsunami response, and location of maximum story drift can be seen in Appendix V.

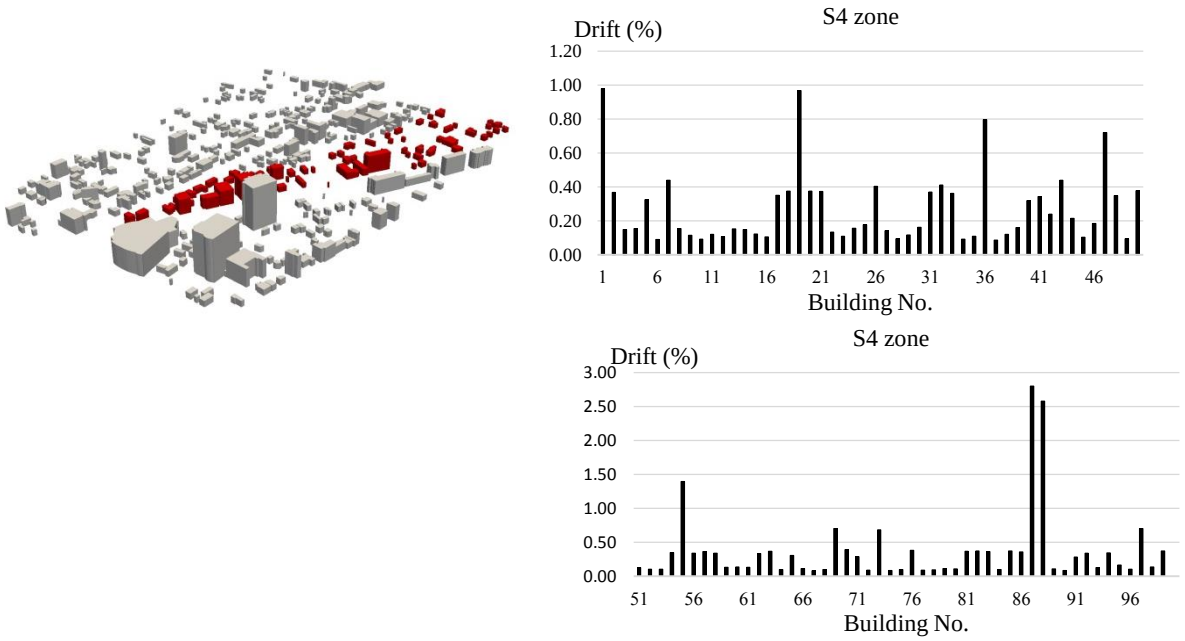

Figure 26: Maximum story drift ratio for zone S4 (worst case)

Figure 26 shows the results of the worst-case scenario for each RC building in zone S4. For each RC building in Figure 26, number of floors, maximum story drift ratio, occurrence during earthquake response or sequential tsunami response, and location of maximum story drift can be seen in Appendix VI.

Table 3 shows number of RC buildings for the worse-case scenario in which maximum story drift ratio occurred during earthquake response and sequential tsunami response. Comparing Table 3 with Table 2 for most of RC buildings, maximum story drift ratio could occur during sequential tsunami response.

Zone	Number of RC buildings	Max drift during earthquake	Max drift during tsunami
N1	50	14	36
N2	51	3	48
N3	114	27	87
S1	31	13	18
S2	56	14	42
S3	76	0	76
S4	99	21	78
Total	477	92 (19.29%)	385 (80.71%)

Table 3 Number of RC buildings for maximum story drift ratio (worst case)

8 CONCLUSIONS

For sequential earthquake and tsunami simulation in the target area of Kochi city, most of RC buildings had maximum drift ratio during earthquake response in which maximum drift ratio was 0.88% for a twenty-one story building in zone S2. In zone S3, many RC buildings had maximum drift ratio during sequential tsunami response in which tsunami inundation depth was a little higher than other zones. For all RC buildings, maximum drift ratio during sequential tsunami response was 0.22% occurred with a three-story building in zone S4 in which structural damage didn't occur obviously. For all zones, three-story buildings had a significant risk that maximum drift ratio could occur during tsunami response analysis.

For the worst-case scenario, most of RC buildings had maximum drift ratio during sequential tsunami response in which maximum drift ratio was 4.71% for a four-story building in zone S3. For all zone, low-rise buildings (three-story to seven-story) had a significant risk that maximum drift ratio was higher than 1% during sequential tsunami response. For the worst-case scenario, structural damage from sequential tsunami response was much more serious than that of the normal-case scenario in which tsunami inundation depth was double.

The results of earthquake and tsunami simulation can be used to designate tsunami evacuation buildings, which must be secured for people living in a surrounding area. These results can indicate a weak point of a city area and focus on this weak point. In addition, these results can be used to construct prevention measures in order control overall damage of a city area from earthquake and subsequent tsunami.

9 APPENDIX

Appendix I The results of damage prediction for zone S2

No.	Floors	Max drift (%)	During	Location
1	1	0.12	T	3
2	1	0.09	E	3
3	2	0.25	E	7
4	1	0.09	E	3
5	1	0.09	T	3
6	1	0.88	E	21
7	1	0.10	T	3
8	1	0.12	T	3
9	1	0.13	T	3
10	1	0.09	E	3
11	1	0.13	E	3
12	1	0.12	E	3
13	1	0.08	E	3
14	1	0.09	E	3
15	1	0.12	E	3
16	1	0.10	E	3
17	1	0.12	E	3
18	2	0.22	E	11
19	1	0.09	E	3
20	1	0.13	T	3
21	1	0.27	E	9
22	1	0.09	E	3
23	1	0.09	E	3
24	1	0.10	T	3
25	1	0.09	T	3
26	1	0.11	E	3
27	1	0.09	T	3
28	2	0.13	E	3

No.	Floors	Max drift (%)	During	Location
29	1	0.14	T	3
30	1	0.08	E	3
31	2	0.15	E	6
32	2	0.09	E	3
33	1	0.14	T	3
34	1	0.09	E	3
35	1	0.14	E	3
36	2	0.11	E	3
37	2	0.17	E	4
38	1	0.10	E	3
39	1	0.08	E	3
40	1	0.14	T	3
41	1	0.11	T	3
42	1	0.15	E	3
43	1	0.09	E	3
44	1	0.10	E	3
45	1	0.11	E	3
46	1	0.10	E	3
47	1	0.09	E	3
48	1	0.11	T	3
49	1	0.08	E	3
50	1	0.10	E	3
51	1	0.12	E	3
52	1	0.11	E	3
53	1	0.14	T	3
54	2	0.13	E	8
55	1	0.23	E	8
56	1	0.15	T	3

Appendix II The results of damage prediction for zone S3

No.	Floors	Max drift (%)	During	Location
1	3	0.15	T	1
2	3	0.09	E	1
3	3	0.11	E	1
4	3	0.11	T	1
5	3	0.10	E	1
6	3	0.19	T	1
7	3	0.15	T	1
8	3	0.11	T	1
9	3	0.14	T	1
10	3	0.13	T	1
11	3	0.12	E	1
12	3	0.12	T	1
13	3	0.10	E	1
14	3	0.21	T	1
15	3	0.11	T	1
16	3	0.12	E	1
17	3	0.13	T	1
18	3	0.12	E	1
19	3	0.12	T	1
20	3	0.10	E	1
21	3	0.12	T	1
22	3	0.15	E	1
23	3	0.09	E	1
24	3	0.11	E	1
25	3	0.14	T	1
26	3	0.08	E	1
27	3	0.16	E	1
28	3	0.11	T	1
29	9	0.18	E	2
30	3	0.11	E	1
31	10	0.21	E	2
32	3	0.10	E	1
33	3	0.15	E	1
34	3	0.12	T	1
35	3	0.11	E	1
36	3	0.12	E	1
37	3	0.14	E	1
38	3	0.12	T	1
39	3	0.14	E	1
40	3	0.12	T	1
41	7	0.20	E	2
42	7	0.17	E	2
43	3	0.12	T	1
44	3	0.11	T	1
45	4	0.16	T	1
46	6	0.23	E	2
47	3	0.14	T	1
48	3	0.11	T	1
49	8	0.19	E	2
50	3	0.15	E	1
51	4	0.13	E	2
52	3	0.14	E	1
53	3	0.14	E	1
54	3	0.09	E	1
55	9	0.24	E	1
56	3	0.10	E	1
57	3	0.16	E	1
58	3	0.09	E	1
59	4	0.16	T	1
60	7	0.17	E	2
61	3	0.10	E	1
62	3	0.12	E	1
63	3	0.12	E	1
64	3	0.14	T	1
65	3	0.18	T	1
66	3	0.12	E	1
67	3	0.19	T	1
68	3	0.11	T	1
69	3	0.19	T	1
70	3	0.13	E	2
71	3	0.11	E	1
72	3	0.16	E	1
73	5	0.21	E	2
74	6	0.25	E	2
75	3	0.13	E	1
76	3	0.15	T	1

Appendix III The results of damage prediction for zone S4

No.	Floors	Max drift (%)	During	Location
1	5	0.18	E	2
2	3	0.10	T	1
3	3	0.10	T	1
4	3	0.11	T	1
5	7	0.16	E	2
6	3	0.09	E	1
7	8	0.22	E	2
8	3	0.11	T	1
9	3	0.12	E	1
10	3	0.09	E	1
11	3	0.11	E	1
12	3	0.10	E	1
13	3	0.11	T	1
14	3	0.10	T	1
15	3	0.12	E	1
16	3	0.10	E	1
17	3	0.12	E	1
18	3	0.13	T	1
19	3	0.14	E	2
20	3	0.13	T	1
21	3	0.10	E	1
22	3	0.12	E	1
23	3	0.11	E	1
24	3	0.15	E	1
25	3	0.13	E	1
26	3	0.14	T	1
27	3	0.12	T	1
28	3	0.09	E	1
29	3	0.09	E	1
30	3	0.11	T	1
31	3	0.14	T	1
32	3	0.15	T	1
33	3	0.14	T	1
34	3	0.09	E	1
35	3	0.09	E	1
36	6	0.25	E	2
37	3	0.09	E	1
38	3	0.12	E	1
39	3	0.16	E	1
40	7	0.18	E	2
41	3	0.09	E	1
42	8	0.24	E	2
43	8	0.21	E	2
44	3	0.11	E	1
45	3	0.10	E	1
46	3	0.13	T	1
47	3	0.16	T	1
48	3	0.15	E	1
49	3	0.09	E	1
50	3	0.14	T	1

No.	Floors	Max drift (%)	During	Location
51	3	0.10	E	1
52	3	0.10	E	1
53	3	0.10	E	1
54	3	0.15	E	1
55	3	0.22	T	1
56	3	0.15	E	1
57	3	0.15	T	1
58	3	0.15	E	1
59	3	0.14	E	1
60	3	0.10	E	1
61	3	0.11	E	1
62	3	0.11	E	1
63	3	0.14	E	1
64	3	0.10	E	1
65	3	0.14	E	1
66	3	0.13	T	1
67	3	0.08	E	1
68	3	0.09	E	1
69	3	0.10	E	1
70	3	0.16	T	1
71	3	0.11	E	1
72	3	0.09	E	1
73	3	0.11	T	1
74	3	0.09	E	1
75	3	0.09	E	1
76	3	0.16	T	1
77	3	0.09	E	1
78	3	0.09	E	1
79	3	0.09	E	1
80	3	0.09	E	1
81	3	0.12	T	1
82	3	0.14	E	1
83	3	0.12	E	1
84	3	0.09	E	1
85	3	0.14	T	1
86	3	0.12	T	1
87	4	0.17	E	2
88	4	0.15	E	2
89	3	0.09	E	1
90	3	0.09	E	1
91	11	0.24	E	2
92	3	0.09	E	1
93	3	0.10	E	2
94	10	0.32	E	1
95	3	0.13	E	1
96	3	0.09	E	1
97	3	0.12	T	1
98	3	0.14	E	1
99	3	0.11	T	1

Appendix IV The results of damage prediction for zone S2 (worst case)

No.	Floors	Max drift (%)	During	Location
1	3	0.28	T	1
2	3	0.10	T	1
3	7	0.36	T	1
4	3	0.12	T	1
5	3	0.13	T	1
6	21	0.88	E	1
7	3	0.14	T	1
8	3	0.17	T	1
9	3	0.29	T	1
10	3	0.26	T	1
11	3	0.17	T	1
12	3	0.14	E	1
13	3	0.08	E	1
14	3	0.09	T	1
15	3	0.12	E	1
16	3	0.46	T	1
17	3	0.47	T	1
18	11	0.22	T	1
19	3	0.09	E	1
20	3	0.29	T	1
21	9	0.33	T	1
22	3	0.09	E	1
23	3	0.11	T	1
24	3	0.14	T	1
25	3	0.13	T	1
26	3	0.13	T	1
27	3	0.28	T	1
28	3	0.13	E	2

No.	Floors	Max drift (%)	During	Location
29	3	0.48	T	1
30	3	0.11	T	1
31	6	0.17	T	1
32	3	0.28	T	1
33	3	0.30	T	1
34	3	0.27	T	1
35	3	0.19	T	1
36	3	0.44	T	1
37	4	1.46	T	1
38	3	0.10	E	1
39	3	0.16	T	1
40	3	0.29	T	1
41	3	0.29	T	1
42	3	0.27	T	1
43	3	0.09	E	1
44	3	0.11	T	1
45	3	0.11	E	1
46	3	0.10	E	1
47	3	0.09	E	1
48	3	0.28	T	1
49	3	0.09	T	1
50	3	0.14	T	1
51	3	0.12	E	1
52	3	0.10	E	1
53	3	0.30	T	1
54	8	0.21	T	1
55	8	0.30	T	1
56	3	0.32	T	1

Appendix V The results of damage prediction for zone S3 (worst case)

No.	Floors	Max drift (%)	During	Location
1	3	0.29	T	1
2	3	0.20	T	1
3	3	0.19	T	1
4	3	0.27	T	1
5	3	0.20	T	1
6	3	0.85	T	1
7	3	0.79	T	1
8	3	0.26	T	1
9	3	0.80	T	1
10	3	0.81	T	1
11	3	0.21	T	1
12	3	0.27	T	1
13	3	0.20	T	1
14	3	1.65	T	1
15	3	0.27	T	1
16	3	0.19	T	1
17	3	0.81	T	1
18	3	0.19	T	1
19	3	0.27	T	1
20	3	0.20	T	1
21	3	0.26	T	1
22	3	0.24	T	1
23	3	0.20	T	1
24	3	0.26	T	1
25	3	0.28	T	1
26	3	0.23	T	1
27	3	0.19	T	1
28	3	0.79	T	1
29	9	0.53	T	1
30	3	0.48	T	1
31	10	0.52	T	1
32	3	0.20	T	1
33	3	0.80	T	1
34	3	0.27	T	1
35	3	0.19	T	1
36	3	0.21	T	1
37	3	0.78	T	1
38	3	0.80	T	1
39	3	0.17	T	1
40	3	0.79	T	1
41	7	1.52	T	1
42	7	0.55	T	1
43	3	0.26	T	1
44	3	0.27	T	1
45	4	4.70	T	1
46	6	2.46	T	1
47	3	0.28	T	1
48	3	0.27	T	1
49	8	0.86	T	1
50	3	0.24	T	1
51	4	2.32	T	1
52	3	0.77	T	1
53	3	0.20	T	1
54	3	0.24	T	1
55	9	0.73	T	1
56	3	0.21	T	1
57	3	0.19	T	1
58	3	0.23	T	1
59	4	4.71	T	1
60	7	0.55	T	1
61	3	0.20	T	1
62	3	0.22	T	1
63	3	0.82	T	1
64	3	0.28	T	1
65	3	0.81	T	1
66	3	0.21	T	1
67	3	0.81	T	1
68	3	0.26	T	1
69	3	0.78	T	1
70	3	0.24	T	1
71	3	0.26	T	1
72	3	0.19	T	1
73	5	3.55	T	1
74	6	2.23	T	1
75	3	0.18	T	1
76	3	0.83	T	1

Appendix VI The results of damage prediction for zone S4 (worst case)

No.	Floors	Max drift (%)	During	Location
1	5	0.98	T	1
2	3	0.37	T	1
3	3	0.15	T	1
4	3	0.15	T	1
5	7	0.33	T	1
6	3	0.09	E	1
7	8	0.44	T	1
8	3	0.16	T	1
9	3	0.12	E	1
10	3	0.09	E	1
11	3	0.12	T	1
12	3	0.11	T	1
13	3	0.15	T	1
14	3	0.15	T	1
15	3	0.12	T	1
16	3	0.11	T	1
17	3	0.35	T	1
18	3	0.38	T	1
19	3	0.97	T	1
20	3	0.38	T	1
21	3	0.37	T	1
22	3	0.13	T	1
23	3	0.11	E	1
24	3	0.16	T	1
25	3	0.18	T	1
26	3	0.40	T	1
27	3	0.14	T	1
28	3	0.09	E	1
29	3	0.12	T	1
30	3	0.16	T	1
31	3	0.37	T	1
32	3	0.41	T	1
33	3	0.36	T	1
34	3	0.09	E	1
35	3	0.11	T	1
36	6	0.80	T	1
37	3	0.09	E	1
38	3	0.12	E	1
39	3	0.16	E	1
40	7	0.32	T	1
41	3	0.34	T	1
42	8	0.24	E	2
43	8	0.44	T	1
44	3	0.22	T	1
45	3	0.10	T	1
46	3	0.18	T	1
47	3	0.72	T	1
48	3	0.35	T	1
49	3	0.09	E	1
50	3	0.38	T	1

No.	Floors	Max drift (%)	During	Location
51	3	0.10	T	1
52	3	0.10	T	1
53	3	0.10	T	1
54	3	0.15	T	1
55	3	0.22	T	1
56	3	0.15	T	1
57	3	0.15	T	1
58	3	0.15	T	1
59	3	0.14	E	1
60	3	0.10	T	1
61	3	0.11	T	1
62	3	0.11	T	1
63	3	0.14	T	1
64	3	0.10	E	1
65	3	0.14	T	1
66	3	0.13	E	1
67	3	0.08	E	1
68	3	0.09	T	1
69	3	0.10	T	1
70	3	0.16	T	1
71	3	0.11	T	1
72	3	0.09	E	1
73	3	0.11	T	1
74	3	0.09	E	1
75	3	0.09	T	1
76	3	0.16	T	1
77	3	0.09	E	1
78	3	0.09	T	1
79	3	0.09	T	1
80	3	0.09	T	1
81	3	0.12	T	1
82	3	0.14	T	1
83	3	0.12	T	1
84	3	0.09	T	1
85	3	0.14	T	1
86	3	0.12	T	1
87	4	0.17	T	2
88	4	0.15	T	2
89	3	0.09	T	1
90	3	0.09	E	1
91	11	0.24	T	2
92	3	0.09	T	1
93	3	0.10	E	2
94	10	0.32	T	1
95	3	0.13	T	1
96	3	0.09	T	1
97	3	0.12	T	1
98	3	0.14	E	1
99	3	0.11	T	1

REFERENCES

[1] M. Hori, S. Tanaka, T. Ichimura, M. Lalith, T. Miyamura, M. Ogino, and S. Okazawa, Application of HPC to earthquake engineering - seismic structure response analysis and urban area earthquake simulation. *4th ECCOMAS Thematic Conference on Computational Methods in Structural Dynamics and Earthquake Engineering*, 1728, 2013

[2] M. Hori, *Introduction to computational earthquake engineering*. 2nd Edition, Imperial College Press, London, 2011.

[3] M. Hori and T. Ichimura, Current state of integrated earthquake simulation for earthquake hazard and disaster. *Journal of Seismology*, Spriger science, 12, 307-321, 2008.

[4] M. Hori, T. Ichimura and K. Oguni, Development of integrated earthquake simulation for estimation of strong ground motion, structural responses and human action in urban areas. *Asian Journal of Civil Engineering (Building and Housing)*, 7, 4, 381-392, 2006.

[5] T. Ichimura, M. Hori, K. Terada and T. Yamakawa, On integrated earthquake simulator prototype: combination of numerical simulation and geographical information system. *Structural Eng./Earthquake Eng.*, JSCE, 22, 2, 233s-243s, 2005.

[6] T. Ichimura and M. Hori, Development of prototype of integrated earthquake disaster simulator using digital city and strong ground motion simulator with high-resolution. *13th World Conference on Earthquake Engineering*, 1418, 2004.

[7] G. Sobhaninejad, M. Hori, and T. Kabeyasawa, Enhancing integrated earthquake simulation with high performance computing. Elsevier, *Advances in Engineering Software*, 42, 286-292, 2011.

[8] M.L.L. Wijerathne, M. Hori, T. Kabeyasawa, and T. Ichimura, Strengthening of parallel computation performance of integrated earthquake simulation. ASCE, *Journal of Computing in Civil Engineering*, 2012.

[9] T. Ichimura, T. Samo, M. Hori, and H. Itami, Integrated earthquake simulator to generate advanced earthquake disaster information. *Internet Journal for Society for Social Management Systems (SSMS)*,2009.

[10] L. Maddegedara and M. Hori, Application of high performance computation for the prediction of urban area earthquake disaster. *Internet Journal for Society for Social Management Systems (SSMS)*, 2011.

[11] D. B. Kirk and W. W. Hwu, *Programming Massively Parallel Processors.* 2nd Edition, Elsevier, Morgan Kaufmann, 2013.

[12] NVIDIA Corporation, *NVIDIA Developer Zone.* 2014

[13] T. Asai, Y. Nakano, T. Tateno, H. Fukuyama, K. Fujima, Y. Haga, T. Sugano, and T. Okada, Tsunami load evaluation based on damage observation after the 2011 Great East Japan earthquake. *Proceedings of the International Symposium on Engineering Lessons Learned from the 2011 Great East Japan Earthquake*, Tokyo, Japan, 2012.